

Doping induced spin-state transition in LaCoO_3 : dynamical mean-field study

P. Augustinský,^{1,2} V. Krápek,^{2,3} and J. Kuneš^{2,*}

¹*Theoretical Physics III, Center for Electronic Correlations and Magnetism,
Institute of Physics, University of Augsburg, D-86135, Augsburg, Germany*

²*Institute of Physics, Academy of Sciences of the Czech republic,
Čukrovarnická 10, Praha 6, 162 53, Czech Republic*

³*Central European Institute of Technology, Brno University of Technology, Technická 10, 616 00 Brno, Czech Republic*

(Dated: August 25, 2018)

The hole and electron doped LaCoO_3 is studied using the dynamical mean-field theory. The one-particle spectra are analyzed and compared to the available experimental data, in particular the x-ray absorption spectra. Analyzing the temporal spin-spin correlation functions we find the atomic intermediate spin state is not important for the observed Curie-Weiss susceptibility. Contrary to commonly held view about the roles played by the t_{2g} and e_g electrons we find narrow quasi-particle bands of t_{2g} character crossing the Fermi level accompanied by strongly damped e_g excitations.

PACS numbers: 75.30.Wx, 71.28.+d, 75.20.Hr, 71.10.Fd

The electron-electron repulsion within the partially filled d shell is for a long time known to place the transition metal oxides among the most puzzling materials with properties varying substantially upon a small change of temperature, pressure, or carrier concentration. More recently the Hund's intra-atomic exchange and the competition between various spin states come to the spotlight as one of the key features in the physics of iron pnictides.^{1,2} However, the spin state competition is a much broader phenomenon³ and we are only starting to understand its implications for the properties of materials.

LaCoO_3 is a prototypical system with competing spin states. A small gap non-magnetic insulator at low temperature acquires Curie-Weiss (CW) susceptibility above 100 K⁴ followed by disappearance of the charge gap between 450 and 600 K.⁵ The generally accepted explanation is essentially atomic physics of the low spin ($t_{2g}^6 e_g^0$) ground state with a nearby excited state of either high spin (HS, $t_{2g}^4 e_g^2$) or intermediate spin (IS, $t_{2g}^5 e_g^1$) character. The nature of the excited state is still debated. Hole doping of the Co d bands by substitution of La with Sr, Ca or Ba also leads to a strong magnetic response.^{6,7} At < 18% Sr concentration microscopically inhomogeneous phase is observed that can be described as magnetic clusters separated by non-magnetic insulating matrix. Above 18% Sr concentrations the material becomes a homogeneous ferromagnetic (FM) metal. The interplay of spin state competition with the itinerant electron physics opens interesting possibilities², which are yet to be investigated.

Properties of $\text{La}_{1-x}\text{Sr}_x\text{CoO}_3$ are commonly discussed in the context of double-exchange model which provides a satisfactory description of related $\text{La}_{1-x}\text{Sr}_x\text{MnO}_3$ family. In this picture the t_{2g} electrons are localized on the metal atom forming the local spin moment while e_g electrons form dispersive bands. Numerous comparative studies, however, found sizeable differences between cobaltites and manganites. Colossal magnetoresistance, the hallmark of manganite physics, is not found in cobaltites.^{6,8} The NMR relaxation rates in cobaltites are several orders

of magnitude larger than in manganites.⁹ The linear specific heat coefficient in $\text{La}_{0.7}\text{Sr}_{0.3}\text{CoO}_3$ is 16 times larger than in $\text{La}_{0.7}\text{Sr}_{0.3}\text{MnO}_3$.⁸ These observations raise the question of the relevance of the double-exchange picture for doped cobaltites.

The strong T -dependence of physical properties even in the parent compound LaCoO_3 make theoretical description of cobaltites challenging. Several density functional and Hartree-Fock calculations on doped cobaltites were reported.¹⁰⁻¹⁴ In this Letter we use the combination of the dynamical mean-field theory¹⁵ and the density functional theory (DFT+DMFT)^{16,17} to study the one-particle spectra and magnetic properties of doped LaCoO_3 . Our results show an evolution with doping from a stoichiometric insulator, where electronic correlations are hidden on the one-particle level, to a FM metal, where a sizable many-body renormalization and quasi-particle (QP) damping take place. The DMFT solutions in the hole-doped regime are characterized by strongly damped e_g excitations and dispersive QP bands of t_{2g} character crossing the Fermi level thus contradicting the double-exchange picture. The local moments which appear upon hole doping are found to originate in the Co HS state.

The calculation proceeds in several steps. First, the LDA band structure is determined using WIEN2k¹⁸ and an effective Hamiltonian spanning the Co d and O p bands is constructed.^{19,24} Although recently doubts have been raised concerning the reliability of $p-d$ model for the Mott-Hubbard systems such as V_2O_3 and LaNiO_3 ²⁰ the strong Co-O hybridization²¹ and its role in stabilization of the LS state²³ suggest that the explicit inclusion of O p states is important for the physics of LaCoO_3 . For all dopings we used the same Hamiltonian obtained for the 5 K lattice parameters of the stoichiometric LaCoO_3 . Adding the explicit electron-electron interaction within the Co d shell we arrive at the multi-band Hubbard Hamiltonian of the form

$$H = \sum_{\mathbf{k}} \begin{pmatrix} \mathbf{d}_{\mathbf{k}}^\dagger \\ \mathbf{p}_{\mathbf{k}}^\dagger \end{pmatrix} \begin{pmatrix} h_{\mathbf{k}}^{dd} - E_{\text{dc}} & h_{\mathbf{k}}^{dp} \\ h_{\mathbf{k}}^{pd} & h_{\mathbf{k}}^{pp} \end{pmatrix} \begin{pmatrix} \mathbf{d}_{\mathbf{k}} \\ \mathbf{p}_{\mathbf{k}} \end{pmatrix} + \sum_i W_i^{dd}. \quad (1)$$

Here, $\mathbf{d}_{\mathbf{k}}$ ($\mathbf{p}_{\mathbf{k}}$) is an operator-valued vector whose elements are Fourier transforms of $d_{i\alpha}$ ($p_{i\gamma}$), which annihilate the Co d (O p) electron in the orbital α (γ) in the i th unit cell. The on-site interaction W_i^{dd} is approximated by the density-density form with parameters $U=6$ eV and $J=0.8$ eV²¹ (for the full interaction matrix see SM). Comparison to the rotationally invariant interaction for similar materials is discussed in Refs. 21,25. To justify the density-density approximation we point out that the presented results hold also in the ferromagnetic phase with broken spin-rotation symmetry as discussed later. The double-counting term E_{dc} approximately corrects for the explicitly unknown mean-field part of the interaction coming from LDA. It was chosen to equal the orbitally averaged Hartree part of the self-energy.²⁶ The hybridization expansion continuous-time quantum Monte Carlo^{27,28} with the improved estimator for the self-energy²⁹ was used to solve the auxiliary impurity problem. All the real-frequency spectra were obtained by analytic continuation of the self-energy using maximum entropy method.³⁰ The calculations were performed at the temperature of 580 K.

The one-particle spectrum of the undoped system²¹ has a character of an uncorrelated band insulator with a gap between the filled t_{2g} and empty e_g states.²² Doping leads to a markedly non-monotonic variation of the orbital occupancies (Fig. 1) indicating a departure from independent particles behavior. In particular on the hole-doped side, approximately two e_g electrons and three t_{2g} holes are created for each hole added to the system. This is accompanied by appearance of fluctuating local moments as reflected by growing spin-spin correlation functions at long times in the absence of static order, $\langle S_z \rangle = 0$ (right panel of Fig. 1).

Before we analyze the origin of the local moments we establish that the result is not an artefact of our choice of the double-counting correction E_{dc} . In addition to the self-consistently adjusted E_{dc} , used throughout the paper (see inset in Fig. 1), we have performed test calculations with E_{dc} fixed to its $x = 0$ value. Fixing E_{dc} moves, with increasing hole doping, the d and p bands towards each other which promotes the LS state. Nevertheless even with E_{dc} varied in the unfavorable direction the observed effect is robust (Fig. 1).

Associating the local moment responsible for CW response of an atom embedded in solid with a particular atomic multiplet may not be possible in a strongly hybridized and even metallic system. In Ref. 21 we have introduced the atomic state correlation matrix $\Pi_{\alpha\beta} = \int_0^{1/T} d\tau \langle P_\alpha(\tau) P_\beta(0) \rangle$ to address this question in undoped LaCoO_3 . $\Pi_{\alpha\beta}$ includes effects of both quantum and statistical fluctuations and provides information about the likelihood of finding the Co atom in state α (column sum) as well as about the average duration of the visit to a given state (large diagonal elements mean long visits). Weighted with the spin matrix elements, $S_\alpha^z S_\beta^z \Pi_{\alpha\beta}$ is the contribution of the pair $\alpha\beta$ to the local susceptibility. The correlation matrix in Fig. 2 reveals that hole doping

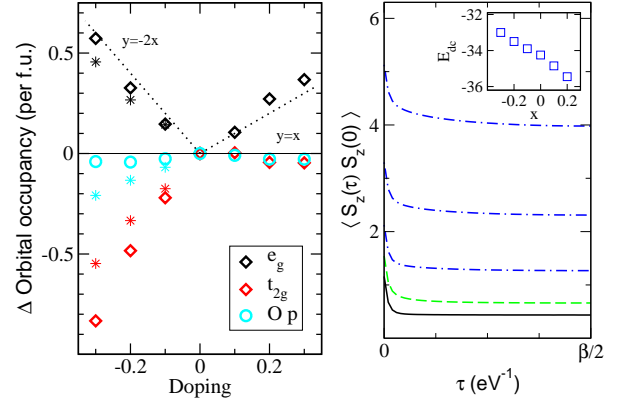


FIG. 1: (color online) Left panel: the doping dependence (hole doping < 0) of the orbital occupancy. The stars mark results obtained with fixed double-counting correction. Considering the FM order for $x=0.3$ changes the data by less than 5%. Right panel: the local spin-spin correlation functions: black (full line) – the undoped system, blue (dash-dotted line) – hole doping $x=0.1, 0.2, 0.3$ (corresponding to increasing magnitude), and green (dashed line) – electron doping of 0.2. The inset shows the doping dependence of E_{dc} .

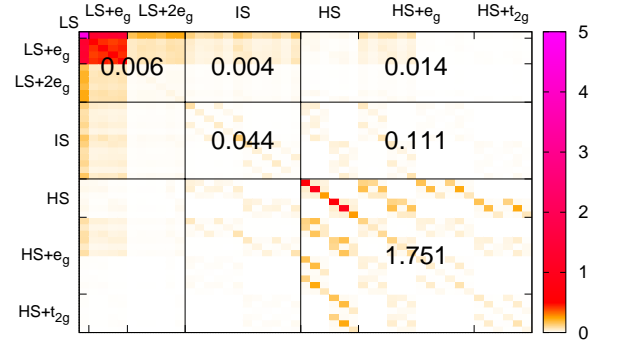


FIG. 2: Atomic state correlation matrix $\Pi_{\alpha\beta}$ for the hole doping of $x=0.2$ with the contribution of the most abundant d^6 , d^7 and d^8 states (see Ref. 21 for the notation). The numbers show the contributions to the local susceptibility $T\chi_{loc}$ summed over the blocks.

causes increasing weight of the HS block which dominates the local susceptibility, similar to the thermal effect in stoichiometric LaCoO_3 .^{21,31}

The one-particle spectral functions decomposed into their momentum and orbital contributions are shown in Fig. 3. The stoichiometric system exhibits sharp bands with well defined dispersion. While the electron doping introduces also some correlation effects we focus on the hole doping which is relevant for $\text{La}_{1-x}\text{Sr}_x\text{CoO}_3$. At $x=0.2$ the chemical potential is pinned close to the top of the t_{2g} band. The e_g spectral weight is transferred from the coherent $e_g - p$ anti-bonding band into incoherent structures around the chemical potential and fills the gap. The k -dependent spectrum clearly shows the

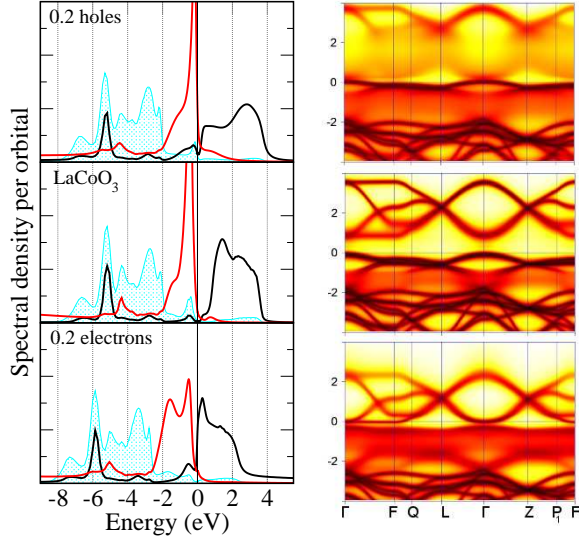


FIG. 3: (color online) Left panel: orbitally resolved spectral density: Co e_g (black), Co t_{2g} (red), O p (shaded blue), $p-\pi$ (lighter blue) for various dopings. Right panel: the corresponding k-resolved spectral functions along the high symmetry lines in the Brillouin zone depicted as color plots.

spectral weight transfer cannot be described as a simple band shift due to an orbitally dependent potential and thus has to be attributed to dynamical correlation effects. With the number of holes growing the chemical potential shifts deeper into the t_{2g} band, which exhibits increasing mass renormalization. At higher doping levels some e_g spectral weight builds up at the chemical potential. These are strongly damped excitations with a lifetime 15 times shorter than that of t_{2g} excitations ($-\text{Im} \Sigma_{e_g}(0) \approx 0.6$ eV, $-\text{Im} \Sigma_{t_{2g}}(0) \approx 0.04$ eV). For the full evolution of the hole doped spectra up to $x = 0.3$ see SM.

The spectral weight redistribution in the conduction band can be observed by the X-ray absorption spectroscopy (XAS). Small core-hole effects at the oxygen K-edge spectrum allow a direct comparison of the XAS data with the O p spectral function, which follows the d spectrum due to $p-d$ hybridization.³² The overall shape of the calculated O p spectrum is unaffected by doping and compares well with the photoemission data of Saitoh *et al.*³³ including the positions of the non-bonding (~ -3 eV) and the σ -bonding peaks (~ -5.5 eV). In Fig. 4 we compare the positive energy part of the O p spectra to the recent experimental data of Medling *et al.*¹³ While the LSDA theory of Medling *et al.* can account for the increase of the low-energy peak while keeping the high-energy peak unchanged upon doping, our LDA+DMFT data reproduce the spectral weight transfer between the two peaks accompanied by appearance of an isosbestic point.³⁴ The increase of the low-energy peak arises from the depopulation of the t_{2g} states as well as from the transfer of the e_g spectral weight, which gradually depletes the high-energy peak.

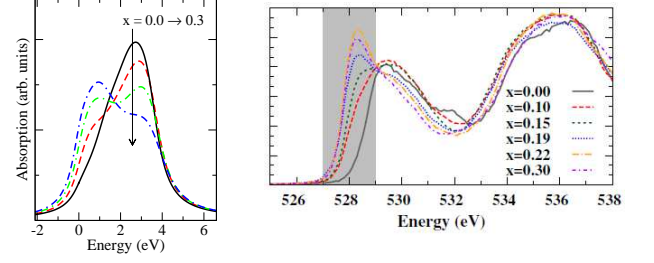


FIG. 4: Left: the unoccupied O p spectra (broadened with Lorentzian) for various hole dopings. Right: The experimental XAS spectra reproduced from Ref. 13.

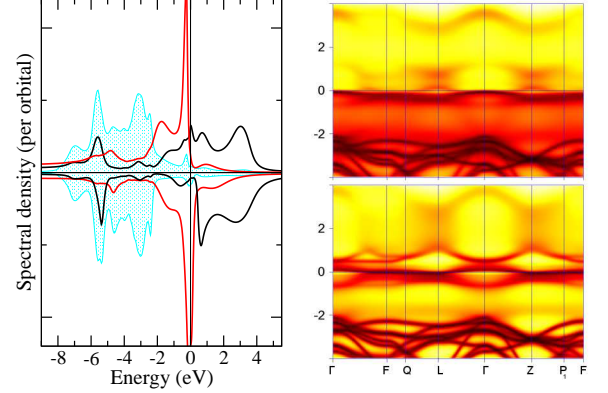


FIG. 5: (color online) Left panel: orbitally resolved spectral density: Co e_g (black), Co t_{2g} (red), O p (shaded blue), $p-\pi$ (lighter blue) for the ferromagnetic solution obtained at $T=580$ K and hole doping $x=0.3$. (Minority spin densities are multiplied with -1). Right panel: The corresponding k-resolved spectra for the majority (top) and minority (bottom) polarization.

Next, we discuss magnetic order. At the hole doping $x = 0.3$ there is a stable FM solution for $T=580$ K. The ordered moment of $1.2 \mu_B$ per formula unit is close to saturation as was confirmed by calculation at lower temperature. This is slightly below the experimental value of saturated magnetization.^{6,35} The spectral functions are shown in Fig. 5. Similar to the spectrum of SrCoO_3 ²⁵, the majority t_{2g} and minority e_g states are absent from the chemical potential, while the minority t_{2g} states form a well defined band, which is the main conduction channel. The majority e_g states form a strongly damped band which crosses the chemical potential. The spin-averaged spectra exhibit only minor difference to the PM spectra, with the e_g lifetime by a factor of two larger in the FM phase (see SM for details). The atomic state correlation matrices show no sizable redistribution of the multiplet weights, in particular no enhancement of the IS block, due to the spin polarization. This shows that inter-site FM correlations $\langle S_i S_j \rangle$, which are completely absent in the PM solution, do not stabilize the IS state.

$\text{La}_{1-x}\text{Sr}_x\text{CoO}_3$ is commonly compared to perovskite manganites and the double-exchange model is invoked

with the partially populated e_g band providing the conduction channel. In this setting the d^6 IS state is a natural building block maximizing the kinetic energy gain. Our results provide a picture which differs in two important aspects: (i) the HS state is identified as the dominant contributor to the CW susceptibility, (ii) t_{2g} QPs are found at the Fermi level while the e_g excitations are strongly damped. In the rest of the paper we discuss our results in the light of the known experimental data.

We studied only homogeneous solutions with full crystal periodicity. The results are, therefore, not relevant for the spin-state polaron regime at very low doping.^{36,37} It is plausible that while IS states participate in the polaron formation they are not important at higher doping levels. The polaron is stable if the kinetic energy gain from delocalizing an e_g electron over the polaron volume outweighs the cost of exciting the participating atoms into the IS state. While the latter term grows linearly with the size of the polaron, the kinetic energy gain is largest for small polarons and quickly saturates as the polaron grows. Therefore only small polarons are stable and a substantial change of magnetic properties around $x = 0.05$ ³⁸ suggests that quite different microscopic physics is involved. Other experimental facts pointing against the IS scenario in the metallic phase ($x > 0.2$) are the lack of substantial magnetoresistance (found in manganites),⁸ no Griffiths phase,³⁹ and observation of positive curvature of inverse susceptibility above T_c .³⁹ The last observation points to increase of the paramagnetic moment with temperature, while in the IS scenario one would expect decrease of IS atoms in magnetically disordered phase.

Instead of the double-exchange mechanism stabilizing the spin-state polarons, which relies on the spin order on nano-scale, we attribute the observed population of the HS state to the hybridization contribution to the crystal field on Co. Introducing a hole on a given Co site is similar to a substitution with a more electronegative element. It results in more covalent bonding with its O neighbors which in turn weakens the covalent bonding between those and the next-neighbor Co atoms promoting the HS states on them.^{40,41} Since the holes are mobile this picture should be viewed only as a simplified static analog of a complex dynamical equilibrium.

Another, perhaps the most important, result is the observation of much stronger damping of e_g excitations than their t_{2g} counterparts. The orbital decoupling^{43,44} by strong J together with closer-to-half filling of e_g orbitals suggests an explanation. However, unlike the system in Ref. 44 our e_g bands do not exhibit an enhanced QP renormalization but rather a pronounced departure from Fermi liquid behavior. We also do not observe a suppression of the inter- or intra-orbital fluctuations (see SM). Therefore we offer a different explanation based on the observation that the effect is still present in the FM solution, where the occupied majority t_{2g} and empty minority e_g orbitals do not play an active role, and that a similar effect (including the behavior of orbital occupan-

cies) is observed⁴⁵ in a much simpler two-band model of Ref. 42 when hole doped. The situation can be viewed as two partially filled asymmetric bands of spinless fermions. The second Born approximation for the self-energy in the imaginary time

$$\Sigma_\sigma(\tau) = U^2 G_\sigma(\tau) G_{-\sigma}(\tau) G_{-\sigma}(\beta - \tau), \quad (2)$$

where $\sigma = \pm 1$ indexes the two bands, shows that the ratio of the self-energies at $\beta/2$ is the inverse ratio of the Green functions. This approximately means that the band with lower density at the Fermi level has more strongly damped QPs. In other words, the slow t_{2g} holes act as ‘static’ scattering centers for the fast e_g electrons, while the t_{2g} holes perceive the e_g electrons as ‘homogeneous gas’.

As a direct consequence of the e_g damping there is only an inverted-U-shaped QP band (t_{2g}) crossing the chemical potential while its U-shaped e_g counterpart is missing, Figs. 3, 5. The prediction of this characteristic spectral feature can be studied with angle-resolved photoemission spectroscopy. Other consequences of the e_g damping, which involve transport coefficients, are less direct allowing only speculative comments at the moment. The present solution is consistent with the absence of colossal magnetoresistance. The anomalous Hall effect observed in FM metallic phase³⁵ may be related to the spin-orbit effects in the t_{2g} QP band crossing the Fermi level. Finally, the contribution of both t_{2g} and e_g channels with different QP damping, of which the e_g one is more sensitive to the magnetic order, should be considered when interpreting the T -dependence of thermopower.⁴⁶

In summary, we have used the dynamical mean-field theory to study hole doping of lanthanum cobaltite. LaCoO_3 is shown to be an example of material in which the electronic correlations are hidden to one-particle spectroscopy at low temperature, but become manifest upon doping. Depletion of electrons from the system leads to growing population of the nominally empty e_g orbitals in striking contrast to the behavior of weakly correlated materials. The LDA+DMFT results provide a good description of the spectral and magnetic properties of the homogeneous metallic phase for $x > 0.2$ where the IS state is shown not to play an important role and the CW susceptibility is attributed to the HS state and fluctuations around it. We found coherent t_{2g} bands crossing the Fermi level, while the e_g excitations are strongly damped and appear at the Fermi level only at dopings $x > 0.2$. This leads to the conclusion that the double-exchange model with the e_g band as the conduction channel is not appropriate for doped cobaltites.

We thank P. Novák, Z. Jiráček, and J. Hejtmanek for numerous discussions. This work was supported by the Deutsche Forschungsgemeinschaft through FOR1346. V.K. was partly supported by European Social Fund, grant No. CZ.1.07/2.3.00/30.0005.

-
- * Electronic address: kunes@fzu.cz
- ¹ Z. P. Yin, K. Haule, and G. Kotliar, *Nat. Phys.* **7**, 294 (2011).
 - ² J. Chaloupka and G. Khaliullin, arXiv:1208.1197.
 - ³ A. Georges, L. de'Medici, and J. Mravlje, *Annual Review of Condensed Matter Physics* **4**, 137 (2013).
 - ⁴ G. Jonker and J. V. Santen, *Physica* **19**, 120 (1953).
 - ⁵ Y. Tokura, Y. Okimoto, S. Yamaguchi, H. Taniguchi, T. Kimura, and H. Takagi, *Phys. Rev. B* **58**, R1699 (1998).
 - ⁶ M. Kriener, C. Zobel, A. Reichl, J. Baier, M. Cwik, K. Berggold, H. Kierspel, O. Zabara, A. Freimuth, and T. Lorenz, *Phys. Rev. B* **69**, 094417 (2004).
 - ⁷ M. Itoh, I. Natori, S. Kubota, and K. Motoya, *J. Phys. Soc. Jpn.* **63**, 1486 (1994).
 - ⁸ M. Paraskevopoulos, J. Hemberger, A. Krimmel, and A. Loidl, *Phys. Rev. B* **63**, 224416 (2001).
 - ⁹ M. J. R. Hoch, P. L. Kuhns, W. G. Moulton, A. P. Reyes, M. A. Torija, J. F. Mitchell, and C. Leighton, *Phys. Rev. B* **75**, 104421 (2007).
 - ¹⁰ M. Abbate, R. Potze, G. A. Sawatzky, and A. Fujimori, *Phys. Rev. B* **49**, 7210 (1994).
 - ¹¹ H. Takahashi, F. Munakata, and M. Yamanaka, *Phys. Rev. B* **57**, 15211 (1998).
 - ¹² P. Ravindran, H. Fjellvåg, A. Kjekshus, P. Blaha, K. Schwarz, and J. Luitz, *J. Appl. Phys.* **91**, 291 (2002).
 - ¹³ S. Medling, Y. Lee, H. Zheng, J. F. Mitchell, J. W. Freeland, B. N. Harmon, and F. Bridges, *Phys. Rev. Lett.* **109**, 157204 (2012).
 - ¹⁴ K. Knížek, Z. Jirák, J. Hejtmanek, and P. Novák, *J. Magn. Magn. Mater.* **322**, 1221 (2010).
 - ¹⁵ A. Georges, G. Kotliar, W. Krauth, and M. J. Rozenberg, *Rev. Mod. Phys.* **68**, 13 (1996).
 - ¹⁶ K. Held, I. A. Nekrasov, G. Keller, V. Eyert, N. Blümer, A. K. McMahan, R. T. Scalettar, T. Pruschke, V. I. Anisimov, and D. Vollhardt, *phys. stat. sol. (b)* **243**, 2599 (2006).
 - ¹⁷ G. Kotliar, S. Y. Savrasov, K. Haule, V. S. Oudovenko, O. Parcollet, and C. A. Marianetti, *Rev. Mod. Phys.* **78**, 865 (2006).
 - ¹⁸ P. Blaha, K. Schwarz, G. K. H. Madsen, D. Kvasnicka, and J. Luitz, *WIEN2K, An Augmented Plane Wave + Local Orbitals Program for Calculating Crystal Properties* (Karlheinz Schwarz, Techn. Universität Wien, Austria, 2001).
 - ¹⁹ A. A. Mostofi, J. R. Yates, Y.-S. Lee, I. Souza, D. Vanderbilt, and N. Marzari, *Comp. Phys. Commun.* **178**, 685 (2008).
 - ²⁰ N. Parragh, G. Sangiovanni, P. Hansmann, S. Hummel, K. Held, and A. Toschi, arXiv:1303.2099.
 - ²¹ V. Křápek, P. Novák, J. Kuneš, D. Novoselov, D. M. Korotin, and V. I. Anisimov, *Phys. Rev. B* **86**, 195104 (2012).
 - ²² The $p-d$ covalency leads to actual occupancies $n_{t_{2g}} = 5.91$ and $n_{e_g} = 0.84$.
 - ²³ M. W. Haverkort, Z. Hu, J. C. Cezar, T. Burnus, H. Hartmann, M. Reuther, C. Zobel, T. Lorenz, A. Tanaka, N. B. Brookes, H. H. Hsieh, H.-J. Lin, C. T. Chen, and L. H. Tjeng, *Phys. Rev. Lett.* **97**, 176405 (2006).
 - ²⁴ J. Kuneš, R. Arita, P. Wissgott, A. Toschi, H. Ikeda, and K. Held, *Comp. Phys. Commun.* **181**, 1888 (2010).
 - ²⁵ J. Kuneš, V. Křápek, N. Parragh, G. Sangiovanni, A. Toschi, and A. V. Kozhevnikov, *Phys. Rev. Lett.* **109**, 117206 (2012).
 - ²⁶ J. Kuneš, D. M. Korotin, M. A. Korotin, V. I. Anisimov, and P. Werner, *Phys. Rev. Lett.* **102**, 146402 (2009).
 - ²⁷ P. Werner and A. J. Millis, *Phys. Rev. B* **74**, 155107 (2006).
 - ²⁸ B. Bauer, L. D. Carr, H. G. Evertz, A. Feiguin, J. Freire, S. Fuchs, L. Gamper, J. Gukelberger, E. Gull, S. Guertler, et al., *J. Stat. Mech.: Theor. Exp.* p. P05001 (2011).
 - ²⁹ P. Augustinský and J. Kuneš, arXiv:1302.4594.
 - ³⁰ J. E. Gubernatis, M. Jarrell, R. N. Silver, and D. S. Sivia, *Phys. Rev. B* **44**, 6011 (1991).
 - ³¹ G. Zhang, E. Gorelov, E. Koch, and E. Pavarini, *Phys. Rev. B* **86**, 184413 (2012).
 - ³² E. Z. Kurmaev, R. G. Wilks, A. Moewes, L. D. Finkelstein, S. N. Shamin, and J. Kuneš, *Phys. Rev. B* **77**, 165127 (2008).
 - ³³ T. Saitoh, T. Mizokawa, A. Fujimori, M. Abbate, Y. Takeda, and M. Takano, *Phys. Rev. B* **56**, 1290 (1997).
 - ³⁴ M. Greger, M. Kollar and D. Vollhardt, arXiv:1212.4980.
 - ³⁵ Y. Onose and Y. Tokura, *Phys. Rev. B* **73**, 174421 (2006).
 - ³⁶ D. Louca and J. L. Sarrao, *Phys. Rev. Lett.* **91**, 155501 (2003).
 - ³⁷ A. Podlesnyak, M. Russina, A. Furrer, A. Alfonsov, E. Vavilova, V. Kataev, B. Büchner, T. Strässle, E. Pomjakushina, K. Conder, et al., *Phys. Rev. Lett.* **101**, 247603 (2008).
 - ³⁸ A. Podlesnyak, G. Ehlers, M. Frontzek, A. S. Sefat, A. Furrer, T. Strässle, E. Pomjakushina, K. Conder, F. Demmel, and D. I. Khomskii, *Phys. Rev. B* **83**, 134430 (2011).
 - ³⁹ C. He, M. A. Torija, J. Wu, J. W. Lynn, H. Zheng, J. F. Mitchell, and C. Leighton, *Phys. Rev. B* **76**, 014401 (2007).
 - ⁴⁰ T. Kyômen, Y. Asaka, and M. Itoh, *Phys. Rev. B* **67**, 144424 (2003).
 - ⁴¹ K. Knížek, J. Hejtmanek, M. Maryško, Z. Jirák, and J. Buršík, *Phys. Rev. B* **85**, 134401 (2012).
 - ⁴² J. Kuneš and V. Křápek, *Phys. Rev. Lett.* **106**, 256401 (2011).
 - ⁴³ L. deMedici, S. R. Hassan, M. Capone, and X. Dai, *Phys. Rev. Lett.* **102**, 126401 (2009).
 - ⁴⁴ Luca deMedici, *Phys. Rev. B* **83**, 205112 (2011).
 - ⁴⁵ J. Kuneš and V. Křápek, (unpublished).
 - ⁴⁶ K. Berggold, M. Kriener, C. Zobel, A. Reichl, M. Reuther, R. Müller, A. Freimuth, and T. Lorenz, *Phys. Rev. B* **72**, 155116 (2005).